Fatigue behavior of ancient masonry arch bridges: residual service life evaluation using stress-life curves method

Michelangelo Laterza[a], Michele D'Amato[b], Vito Michele Casamassima[c]
[a,b,c] *DICEM – Dept. of European and Mediterranean Cultures: Architecture, Environment and Cultural Heritage. University of Basilicata, 75100 Matera, Italy.*

Keywords: fatigue behavior, masonry arch bridge, stress-life, service life, serviceability limit.

ABSTRACT
The conservation and safety assessment of old masonry arch bridges represent nowadays a research field of considerable interest. Most of them are testimonies of the past with a significant historical and cultural value, and represent nowadays, a large part of the transport infrastructures serving strategic link for roads and railways networks. In many cases, their masonry primary elements are already deteriorated due to weather conditions and to the effects of cyclic traffic loads that are increased in both the frequency and the intensity with respect to the past.
Even if the ultimate load is not reached, the cumulated damage along with the localised deterioration can reach levels not acceptable, leading to the out of service of the entire structure.
In this paper, different models are applied in according to the stress-life curve method for estimating the fatigue strength and residual service life of a case study, an Italian ancient multi-span masonry arch bridge still in service.

1 INTRODUCTION

The old masonry arch bridges represent an important infrastructural heritage asset. Masonry arch bridges are an established part of rail and rail infrastructural network. One of the actual engineering challenges is represented by the conservation of very old masonry arch bridges.

It is estimated that there are approximately one million masonry arch bridge spans currently in service around the world. Recent study report that are over 220,000 railway bridges in Europe, of which over 35% are more than 100 years old with a further 31% aged between 50 and 100 years. Out of all European railway bridges 60% are masonry, 23% concrete, 22% metallic. Their bearing capacity strictly depends on the actual structural maintenance, that in many cases is not adequate for contrasting material deterioration and consequent integrity lost, accelerated as well by the environmental conditions and the cyclic load. To date few experimental tests have been performed on existing multi-span brick arch bridges or on scaled prototypes. These studies, conducted by considering both service and ultimate conditions, have revealed some important issues on the structural behavior of this bridge typology. For these bridges it is important to know, in addition to the ultimate vertical load, the maximum service load, that is the traffic load beyond the which the accumulated fatigue damage level into the elements becomes not acceptable and, consequently, the bridge results out of service. These studies, conducted by considering both service and ultimate conditions, have revealed some important issues on the structural behavior of this bridge typology.

Sudden bridge failure or collapse does not only endanger human lives, but also have great economic and environmental consequences, e.g. associated repair costs, road closures, diversions. Very often they were built in last centuries and nowadays are exposed to different vehicular.

2 FATIGUE EXPERIMENTAL TESTS

Few experimental tests have been contucted to the aim to investigate the behavior of masonry under repeated normal stresses.

The tests, conducted on brick masonry specimens, have had the aim of establishing the stress-life curves (S-N curves, for brevity), where the alternating normal stress amplitude (S_a), or

else the maximum normal stress (S_{max}), is being represented as function of the imposed cycles number (N) up to the specimen failure.

Three considered models are examined and compared among them.

Ronca et al. (2004) performed a series of experimental tests on a number of small-scale masonry specimens. The specimens were cast with a mortar of M4 class in conformity with BS EN998-2 (2003) requirements, and using brick blocks with the average strength in compression of 48.86 N/mm^2. The resulting masonry had an average ultimate strength in compression ranged between 10 and 13 MPa. The brickwork prisms were tested under very high vertical loads axially applied (65-80% of the ultimate compressive strength), and by imposing a small variation of the alternating loads having three different frequencies: 1, 5, and 10 (Hz). The Table 1 reports derived details of all tests conducted where: S_{max} and S_{min} are respectively the maximum and the minimum stress in the cycle, S_a the stress induced to the alternate load, S_u the ultimate compressive strength of masonry and R the stress ratio of S_{min} to S_{max}. In Figure 1 are plotted the experimental stress-life curves in terms of logN versus S_a/S_u as reported by the authors, and in the derived form logN versus S_{max}/S_u (Figure 2). Tests details and results published by Ronca et al. (2004).

Table 1. Masonry parameters investigated by Ronca et al. (2004).

N° of samples	f (Hz)	R=Smin/Smax	S=Smax/Su	Sa/Su
3	1	0,78	0,90	0,1
3	1	0,83	0,88	0,075
3	1	0,88	0,85	0,05
1	1	0,73	0,75	0,10
2	5	0,73	0,75	0,10
1	10	0,83	0,70	0,05

In Roberts et al. (2006) a series of fatigue tests on the brick masonry specimens were carried out with the aim of defining the link between fatigue strength of brick masonry and the one of arch bridges. They investigated the influence of stress gradient and saturation degree on the quasi-static and high-cycle fatigue strength of brick masonry. The tests were conducted on three types of test specimens for simulating more closely the masonry arch barrels, and considering as well as both dry and saturated conditions.

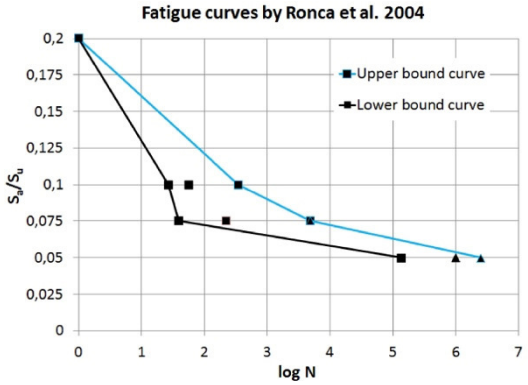

Figure 1. Ronca et al (2004) fatigue curves: experimental data published by authors

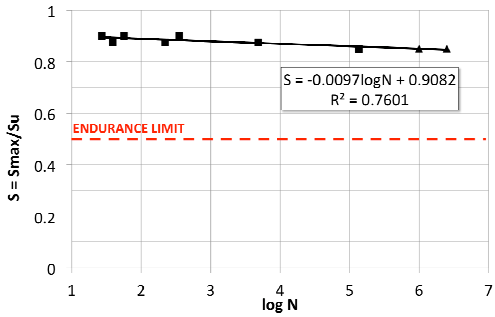

Figure 2. Ronca et al. derived diagram in the form of log N-S.

Vertical load eccentricity ratios e/d ranged from 0 to 0.256 (where e is the vertical load eccentricity and d the specimen depth) were applied. During all tests the load frequency was typically kept constant to 5 Hz until the failure. The test series indicated that the high cycle fatigue strength of wet and submerged brick masonry specimens was only slightly less than the one of dry specimens. The mortar was mixed in order to reproduce the representative mortar used for ancient brick masonry arches. It showed a compressive strength measured at 28 days ranged between 0.45 MPa and 2.78 MPa. The masonry compressive strength determined by assuming a linear stress distribution along the specimens varied between 6 and 14 N/mm^2. The authors proposed the following induced stresses function F(S) for describing the fatigue resistance of masonry specimens:

$$F(S) = \frac{(\Delta S \cdot S_{max})^{0,5}}{S_u} = 0.7 - 0.05 \log N \qquad (1)$$

where S_{max} is the maximum induced stress, ΔS is the induced stress range calculated as the difference between S_{max} and S_{min} (the minimum induced stress), and S_u is the quasi-static masonry compressive strength. In particular, for dry, wet and submerged brick masonry the F(S) was

proposed as lower bound curve of all fatigue strengths experimentally evaluated Eq.(1).

By introducing in the Eq. (1) the stress ratio $R=S_{min}/S_{max}$, and substituting to ΔS the difference $S_{max}-S_{min}$, the fatigue curve F(S) may be rewritten in the familiar form of stress-life curve logN-S_{max}/S_u:

$$S = \frac{S_{max}}{S_u} = \frac{1-0.05\log N}{\sqrt{1-R}} \qquad (2)$$

In the Eq. (2) the fatigue strength S depends only on the imposed number of cycles N and on the amplitude of the induced stresses range R (the lower the R ratio the higher the interval amplitude of stresses). In Figure 3 are plotted the stress-life curves obtained with the Eq. (2) by varying the stress ratio R from 0 to 0.9.

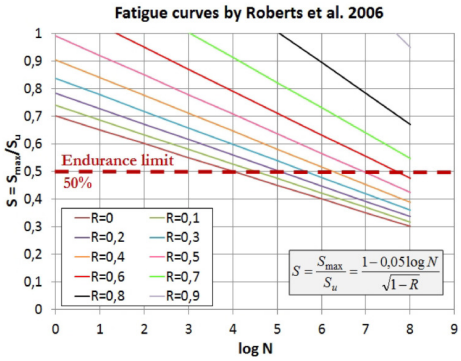

Figure 3. Derived S-N curves from Robert et al. 2006

It is easy to note that the fatigue strength S, for a given value of R, linearly decreases with the logarithm of the maximum number of the imposed cycles N. Moreover, for a given number of the imposed cycles, the higher the fatigue strength (S) the lower the interval amplitude of the induced stresses (that is R increases). Starting from the experimental data obtained by Roberts et al. (2006), Casas (2009) suggested new fatigue curves derived with a probabilistic approach. By using the Weibull distribution function, widely used for the analysis of metals and extended to concrete elements, the following fatigue equation was proposed for describing the progressive fatigue deterioration of brick masonry:

$$S = \frac{S_{max}}{S_u} = AN^{-B(1-R)}, \quad S \geq 0{,}5 \qquad (3)$$

where the fatigue parameters A and B are depending on the assumed survival probability, and S=0.5 is the endurance limit observed according to the work of Melbourne et al. (2004). In the case of a survival probability of 95% (i.e. 5% of probability of failure) and for specimens in any condition (dry, wet, and submerged) the following equation was proposed:

$$S = \frac{S_{max}}{S_u} = 1{,}106N^{-0{,}1034\cdot(1-R)}, \quad S \geq 0{,}5 \qquad (4)$$

The stress-life curves obtained with the Eq. (4) are shown in Figure 4 for different values of the stress ratio R, together with the endurance limit.

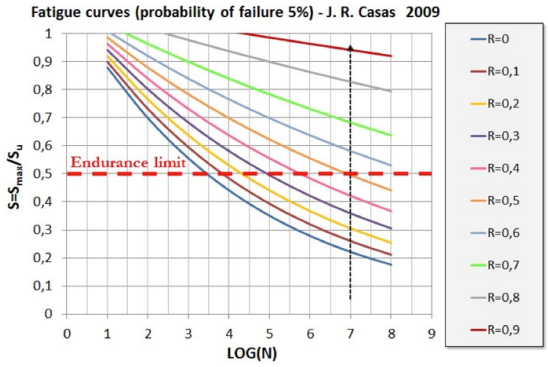

Figure 4. Casas (2009) fatigue curves, referred to a 5% of failure probability

It is clear to note that, with a nonlinear relationship, the fatigue strength S reduces by increasing the maximum number of the imposed cycles N. Conversely, for a given number of the imposed cycles N, the fatigue strength increases if the interval amplitude of the induced stresses (R) decreases (that is ratio R increasing).

3 COMPARISONS AMONG THE CONSIDERED STRESS-LIFE CURVES

In Figure 5 are illustrated in the semi-logarithmic plane Log N-S the comparisons among the stress–life curves examined in this work, by referring to the following values of the ratio $R=S_{min}/S_{max}$: 0, 0.2, 0.4, 0.6, and 0.8. Moreover, the curves proposed by Casas (2009) are drawn by referring to 95% survival probability. This value, corresponding to the 5% lower fractile, is indicated by the considered codes in this study (EC3 and NTC-08 code) as the nominal compressive strength of a material. Also, in the same figure is plotted the linear stress-life curve proposed by Ronca et al. (2004) related to the ratio R equal to 0.8, since 0.8 is approximately the average value of the imposed R in all the performed tests. Finally, in all the graphs the fatigue endurance limit S=0.5 is indicated, too.

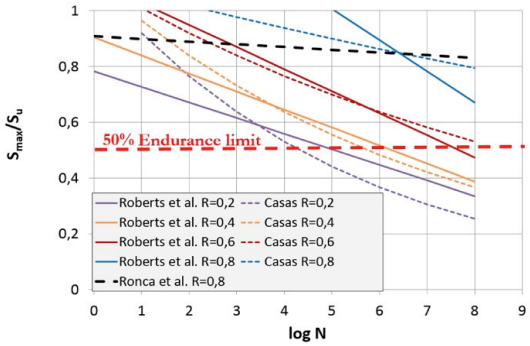

Figure 5. Comparison among the stress-life curves considered from different values of R.

In the comparisons it is clear to note that the scatter between the Roberts and Casas diagrams significantly reduces for the ratios R equal to 0,4 and 0,6, while for the other considered ratios R (0, 0,2 and 0,8) the differences are being more evident. Furthermore, in the case of the Ronca model the curves provide values of the same order of the other models. It is important to outline that all the considered models may predict very low cycles number at failure, even for a stress level corresponding to the classic endurance limit.

4 FATIGUE ASSESSMENT OF AN ANCIENT MULTI SPAN MASONRY ARCH BRIDGE

In this paper is performed the fatigue assessment of an ancient multi-span masonry arch bridge built in Italy before the Second World War and actually still in service. The bridge, called "Cavone Bridge" takes the name from the crossing river, and consists of seven arches of brick masonry having an overall length of 140 m, with a width of 5.6 m. More in detail, the bridge has four secondary arches of 10 m span length, and three main arches of 22 m span length. The latter are supported by two piers falling into the riverbed, having a total height from the foundation plane of about 24 m, of which 14 m are outside the riverbed. Actually, the bridge is serving a provincial road in according to the Italian Transport Classification (1992).

The bridge was interested by some in situ tests addressed to identify the typology and the thickness of all the elements. The tests highlighted that the piers, abutments and spandrel walls consist of an external leaf of regular stone blocks. The piers have a core of cohesive backfill, while the bridge deck is formed by an incoeherent backfill having the function of spreading the traffic loads to the supporting arches. The bridge geometrical schematization is reported in Figure 6, while in Figure 7 are illustrated some images of the bridge.

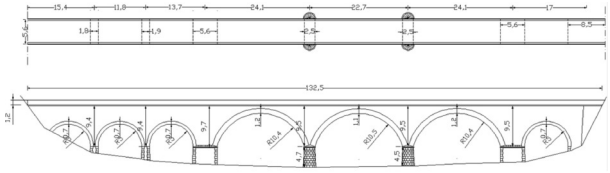
Figure 6. Geometrical schematization of the bridge.

Figure 7. Some photos of the Cavone Bridge.

To date neither in-situ nor laboratory tests have been performed for evaluating the masonry strength. Therefore, the reference values of mechanical properties indicated in the Italian Design Code Instructions (2009) for masonry are assumed in the numerical analyses. More precisely, two different material knowledge levels are supposed (Eurocode8 2004, Italian Design Code Instructions 2009): a limited knowledge level (KL1), and a full knowledge level (KL3). For both the considered knowledge levels the assumed values are hereinafter discussed. Recently the bridge main arches of the bridge have been strengthened by continuous uniaxial carbon fibers (CFRP wraps) applied at the intrados through the wet layout technique, in order to improve the resistance against the vertical moving loads. The details of the applied CFRP wraps are reported below.

As previously stated in the Introduction section the fatigue assessment discussed in this paper regards only the bridge arches by assuming, because of the actual degradation conditions, that their fatigue resistance is attained when the damage accumulation exceeds a tolerance limit, without a global failure occurrence involving piers and spandrel walls. This fatigue assessment criterion is allowed by the considered EC3 (2003) and NTC-08 (2008) codes. The bridge arches here studied may be grouped into two different typologies: the main arch (three in total) having 22 m span length, and the secondary arch (four in total) of 10 m span length.

The first aspect to be discussed is the traffic load to consider. It is known that the stress

spectrum induced within the arches is depending on the vehicles geometry, axle loads, vehicle spacing, composition of the traffic and its dynamic effects. In this study the fatigue load named Fatigue Load Model 3 is considered since, as suggested in EC1 (2003) and NTC-08 (2008), it is more appropriate for typical heavy traffic on European main roads or motorways, and also is coherent with the importance of road served by the considered bridge. In detail, the Fatigue Load Model 3 is schematized through four axles, each of them having two identical wheels. The weight of each axle is equal to 120 kN, and each wheel has a square contact surface of 0.40 m x 0.40 m. Each couple of axes has a distance of 1.20 m, while the distance between the two internal ones is 6.00 m. The geometric schematization of the load is reported in Figure 8.

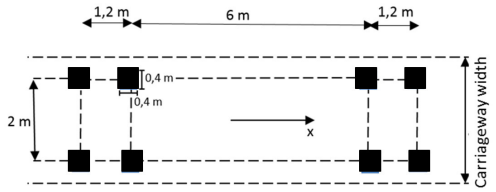

Figure 8. Scheme of Fatigue Load 3 adopted for the fatigue assessment in accordance with EC1 and NTC-08.

Also, it is reasonable to assume that the road served by the bridge is interested by a traffic category of Type 2, in according to EC1 (2003) and NTC-08 (2008) code. Therefore, the number Nobs of heavy vehicles expected per year and per slow lane is assumed equal to 0.5×10^6 according to NTC-08(2008).

It must be pointed out that many of the actual design codes, among which the EC3 and the Italian NTC-08 considered in this work, do not provide any indication about the fatigue strength of masonry elements. Admittedly, attention is only paid to steel elements where methods and stress-life curves are provided for assessing the fatigue resistance. Therefore, it has assumed that the procedure hereinafter applied follows the one proposed in the EC3 and NTC-08 for steel elements, but by applying specific stress-life curves for masonry material. In accordance with this procedure, the stress range $\Delta\sigma i$ (due to the stress fluctuation resulting from the transit of the load model along the arch) is amplified by γ_{Ff}, that is the partial factor for equivalent constant amplitude stress range $\Delta\sigma i$. Whereas, the fatigue strength S is divided by the fatigue strength partial factor γ_{Mf} for obtaining, from the factored stress-life curve, the endurance value N_{Ri}. The entire cumulated damage during the design life of the examined arch may be calculated from the following equation:

$$D = \sum_{i}^{n} \frac{n_{Ei}}{N_{Ri}} \tag{5}$$

where n_{Ei} is the cycles number associated with the stress range $\gamma_{Ff}\Delta\sigma i$ (for band i) in the factored spectrum expected in a certain period (for example the service life); N_{Ri} is the fatigue endurance (in cycles) obtained with the factored stress-life curve $\Delta\sigma c / \gamma_{Mf}$ - N_R for the known stress range of $\gamma_{Ff}\Delta\sigma i$. The partial factor for fatigue strength γ_{Mf} takes into account the consequence of the failure and the used design assessment, while γ_{Ff} is a partial factor for equivalent constant amplitude stress range. In this study, it is assumed that high consequence of failure arises when the fatigue material strength is reached. This is due to the fact that the arches have a low damage tolerance because of masonry degradation, that significantly compromises their integrity and robustness. Therefore, γ_{Mf} is assumed equal to 1.35, while the γ_{Ff} partial factor is assumed equal to 1.0 according to Eurocode 3 (2003). The Eq.(5) represents a linear damage accumulation summation, known also as Palmgren-Miner rule. It expresses the entire cumulated damage in the examined element when repeated vehicles load transit along the bridge. In according to this rule, the fatigue failure occurs when the summation of the so-called cycle ratios (n_{Ei}/N_{Ri}) is equal to one.

The induced stress range $\Delta\sigma i$ due to vehicle transit is evaluated starting from to the combination of permanent loads, that are in this case the self-weights of arches, of backfill and road pavement. The backfill passive pressure is as well taken into account with the classical assumption that the magnitude of the horizontal backfill pressure is proportional to the vertical weight pressure exerted by the backfill material, in according to the work of Gelfi (2002).

The fatigue verification is conducted for the most unfavourable position of the moving load for the normal stresses within the arches. In this work, two different sections are monitored for each arch: the key and the haunch section. It is supposed that the concentrated wheels load spreads from the vertical up to the arches extrados with a dispersal angle assumed equal to 45°, since no information is available about the backfill consolidation (EC1, 2003).

Transversally, with this angle the entire bridge width results involved and, therefore, the problem may be considered plane. In Figure 9 are depicted the most unfavourable positions found for the fatigue load model and the equivalent distributed traffic load calculated as follows:

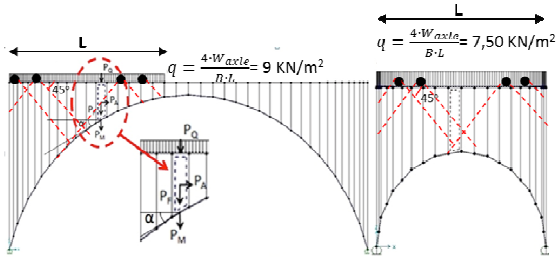

Figure 9. Fatigue load scheme of secondary and main arch referred to the most unfavorable position of the moving load.

where W_{axle} is weight of each axle (equal to 120 kN), B is bridge width, and L is the length of spreading on the arch extrados. In order to investigate the stress state within the main and secondary arch two different numerical models have been implemented into OpenSees (2009), by using rectilinear fibers beams having the unit width section reported in Figure 10.

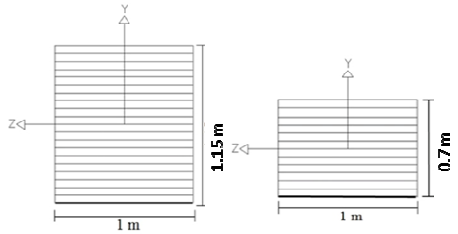

Figure 10. Fibers sections of the main arch and of the secondary arch.

Analyses methods based on plane section assumption may be found also in Chen (2002), and CNR-DT 200/R1 (2013). The masonry material has been modelled with an uniaxial elastic-perfectly plastic relationship (Figure 11) having strength only in compression, with infinite ductility for avoiding solution convergence problems during the numerical simulations. As it will be shown later, this assumption will not influence the arches response under fatigue loads, since the normal stresses never achieve the material strength in all the performed analyses. On the other hand, the infinite ductility will permit of evaluating, in the case of main arch typology, the ultimate carrying load although this assumption may lead, as demonstrated in de Felice, (2009), to an overestimation of the actual arch capacity. However, for the aim of this work this assumption is considered acceptable.

The effects due to the application of the local strengthening with uniaxial Carbon FRP wraps (CFRP) has been numerically investigated, too. For completeness, in this study it has been supposed that the CFRP wraps are applied either at intrados or extrados for both the arch typologies. In general, the intradosal reinforcement is easier to realize since it may be locally applied from the arch bottom without any interruption of bridge viability. On the contrary, the extradosal application may be performed when a global upgrading intervention is planned, implying also the pavement and backfill removing, with a consequent interruption of bridge viability. Whereas, the extradosal application provided a significant ductility rather resistance before the collapse.

The CFRP wraps are supposed to be completely bonded with resin and continuously applied along the width and the longitudinal length of the arch, starting from the impost. They have a Young's modulus of 230000 MPa, a rupture tensile strength of 4800 MPa and, in this study, a total thickness of 0.33 mm (two layers of CFRP). The reinforcement has been modelled as an additional layer with an elastic uniaxial stress-strain law only in tension, having an axial strength fdd evaluated in accordance with CNR-DT 200/R1 (2013), and corresponding to the debonding failure from the masonry support. In this study, the fdd strength is equal to 316 MPa. After reaching the maximum strength fdd the CFRP material law suddenly reduces (Figure 12), for simulating the fibers detachment invalidating the plane section assumption. As regards as the masonry compressive strength is concerned, the following values are assumed for the two simulated knowledge levels:

- Limited Knowledge Level (KL1): the mean value of masonry compressive strength assigned to arches results equal to 2.40 MPa (the minimum value of the interval of strength indicated by NTC-08 Instructions, 2009). The confidence factor CF is equal to 1.35 for reducing the strength considered;
- Full Knowledge Level (KL3). The compression strength assigned to arches is supposed to be equal to 3.20 MPa, corresponding to the mean value of the interval of strength indicated by the same Instructions. In this case the confidence factor CF is equal to 1.00. The material properties assumed in the performed

numerical analyses.are assumed according to the NTC-08 Instructions, 2009).

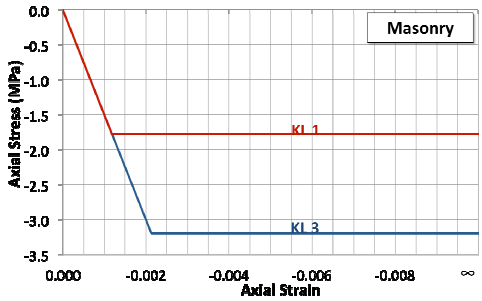

Figure 11. Uniaxial stress-strain relationships assigned to the fibers of masonry.

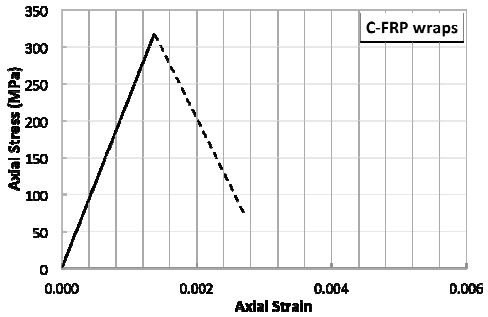

Figure 12. Uniaxial stress-strain relationships assigned to the fiber of CFRP wraps.

5 NUMERICAL RESULTS

For brevity of exposition in Figure 13 and Figure 14 are reported, for the two considered arch typologies, only the most unfavorable results obtained with the numerical simulations. They are obtained by referring either to the current condition (column "Without Wraps") or by considering the application of the CFRP wraps placed either at intrados or extrados (table columns intradosal or extradosal wraps). For both the simulated knowledge levels (KL1 and KL3), it has been found that the most stressed sections result the haunch and key sections of the main and the secondary arch, respectively. In Figure 13 and Figure 14 are also shown the obtained S ratios. For sake of comparison, in the same graph the endurance limit (drawn with a dashed line) is plotted, too. It must be remarked that for both the considered knowledge levels no important variation is produced by CFRP wraps on the most unfavorable stress state.

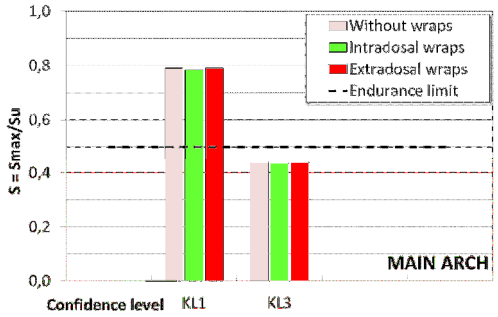

Figure 13. S_{max}/S_u ratios obtained by varying the knowledge level of the main arch.

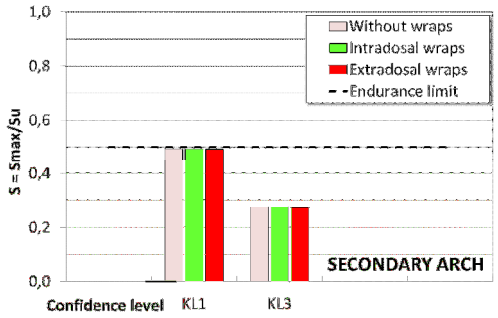

Figure 14. Smax/Su ratios obtained by varying the knowledge level of the secondary arch.

This means, in other words, that the reinforcement does not change the response of the two arches with respect to the considered traffic loads (that is the serviceability limit state of fatigue). Moreover, it is easy to note that the normal stresses are always lower than the material strength and, therefore, the stresses fluctuation arises always in the elastic field.

In order to perform the fatigue assessment of the two arches, in Figure 15, Figure 16 and Figure 17 are reported the stress-life curves proposed by Ronca et al. (2004), Roberts et al. (2006) and Casas (2009), as well as the factored ones (with dashed lines) derived by applying the factor γ_{Mf} in compliance with by NTC-08 (2008) and EC3 (2003) codes. In the same figures are also depicted (with continuous horizontal lines) the ratios S (S_{max}/Su) obtained with the numerical simulations. As it is clear to notice, all the S_{max}/S_u ratios, except for the ones of the main arch in the case of KL1, result always less than the ratio S=0.5, usually indicated as the fatigue endurance limit.

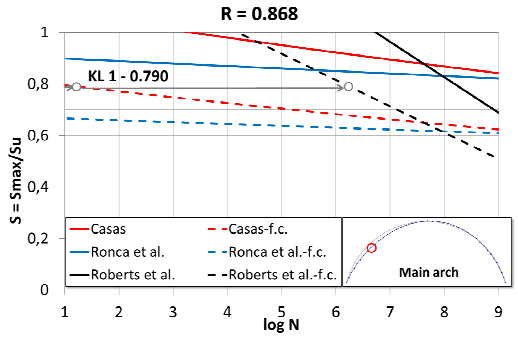

Figure 15. Main arch : calculation of the life cycles at the failure. The factored curves (f.c.) with coefficient R = 0,868 are plotted with a dashed lines.

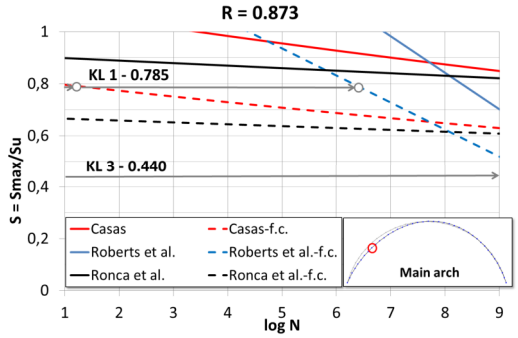

Figure 16. Main arch: calculation of the life cycles at the failure. The factored curves (f.c.) with coefficient R = 0,873 are plotted with a dashed lines.

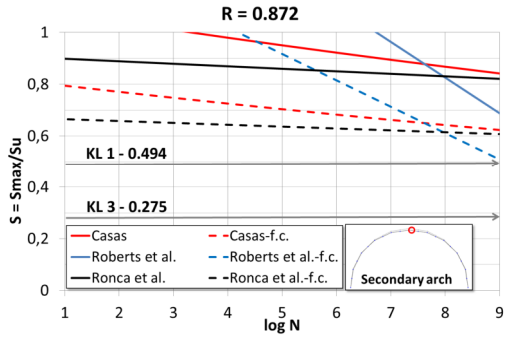

Figure 17. Secondary arch: calculation of the life cycles at the failure. The factored curves (f.c.) with coefficient R =0,872 are plotted with a dashed lines.

In these cases the number of load cycles N at the material failure would result greater than 10^9 with a substantially infinite residual service life. In fact, by assuming a number N_{obs} equal to $0.5x10^6$ corresponding to the heavy vehicles passing per year for the considered road traffic category, the residual life given by the expression:

$$\text{Residual life} = \frac{N}{N_{obs}} \qquad (6)$$

would result greater than 2000 years. In the Eq. (6) N is the cycles number related to the fatigue failure, and Nobs are the passages expected on the road associated with the assumed traffic category. Conversely, as regards for the main arch with a KL1, a very low residual life is obtained by using the fatigue curves proposed by Roberts et al. (2006) and Casas (2009). Whereas, the Ronca et al. (2004) model is inapplicable because of the ratios S_{max}/Su are always greater than the factored curve. Thus, for this model no evaluation of the residual life may be performed. In Table 2 are summarized the calculated residual lives. It is worth to note that the in the case of the main arch the estimated residual life results comprised about from zero (in all configurations with the Casas model) up to more than 5 years (in the case of intradosal CFRP wraps application with the Roberts et al. model). It is easy to note that the CFRP wraps do not produce significant increment of the residual life.

Table 2. Residual service life of the main arch in the case of knowledge level KL1

Without CFRP wraps R = 0,868

S-N curves	Log(N)	N	Smax/Su	Residual life (years)
Casas (2009)	1,17	14,63	0,791	≈ 0
Robert et al. (2006)	6,25	1780025,21	0,790	3,56

With extradosal CFRP wraps R = 0,868

S-N curves	Log(N)	N	Smax/Su	Residual life (years)
Casas (2009)	1,17	14,63	0,791	≈ 0
Robert et al. (2006)	6,25	1780025,21	0,790	3,56

With intradosal CFRP wraps R = 0,873

S-N curves	Log(N)	N	Smax/Su	Residual life (years)
Casas (2009)	1,48	30,41	0,785	≈ 0
Robert et al. (2006)	6,25	2797211,26	0,785	5,59

However, it must be pointed out that generally the intervention with CFRP wraps is applied as local strengthening for improving the ultimate carrying capacity of an arch. The effectiveness of this reinforcement is strictly related to the wraps debonding strength that may take place very early if the connection with the masonry support is not strong enough. Simplified relations and relevant informations concerning detachment of the CFRP wraps may be found, among the others, in Foraboschi (2004). By contrast, if one considers

that along the whole intrados length no debonding is permitted, the arch collapse occurs by compressive failure of the masonry, and the ultimate load is considerably increased. For sake of completeness, in this work it is useful to evaluate as well the ultimate carrying capacity of the reinforced main arch, whose fatigue assessment has been also previously evaluated in the case of KL1. The investigations are performed by varying the debonding strength between the FRP wraps and the masonry support. In doing so, three different values of uniaxial strength fdd are supposed: fdd=316 MPa related to the actual anchorage conditions, f_{dd}=158 MPa (i.e. half of the actual one), and f_{dd}= 4800 MPa corresponding to the CFRP wraps uniaxial tensile strength (i.e. debonding does not occur).

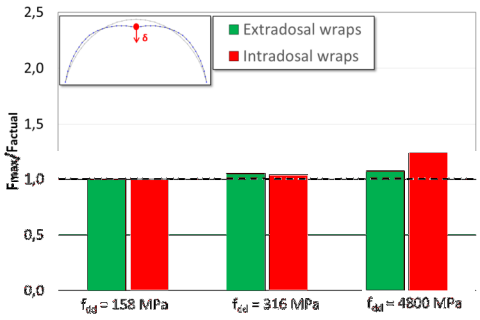

Figure 18. – Main arch: different ratios of F_{max}/F_{actual} obtained at the key.

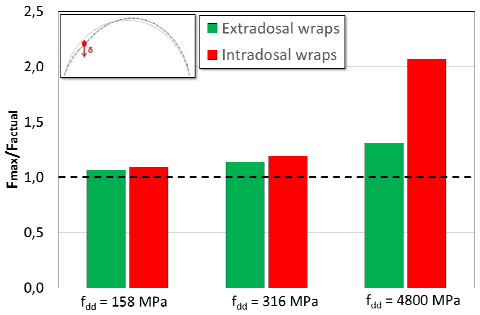

Figure 19. – Main arch: different ratios of F_{max}/F_{actual} obtained at the haunch section.

The numerical simulations are conducted by imposing an increasing monotonic displacement in correspondence of the key and haunch sections (where the most unfavourable stresses for fatigue are obtained), until the arch failure. In Figure 18 and Figure 19 are reported the values of the obtained ratios F_{max}/F_{actual}, where Fmax is the maximum arch carrying capacity with CFRP wraps, and F_{actual} the corresponding one without CFRP wraps (i.e. in the actual condition). These ratios are referred to both the monitored sections (haunch and key section) for the three values of debonding strength f_{dd}. Again, one can easily observe that, if the premature FRP wraps debonding is prevented, a significant benefit in terms of strength is obtained only in the case of intradosal application (the resultant strength, in this case, is doubled).

6 CONCLUSIONS

In this paper the stress-life curve method has been applied for fatigue assessment of ancient brick masonry arch bridges. In particular, different fatigue curves have been considered for evaluating the damage accumulation due to traffic load, in compliance with the procedure proposed by the EC3 (2003) and NTC-08 (2008). Since in the examined codes no clear indication is reported for masonry elements, the fatigue performance approach has been applied similarly to the one proposed for steel elements. By applying this analogy, three different stress-life curves have been considered, in accordance with the models proposed by Ronca et al. (2004), Roberts et al. (2006), and Casas (2009). To date, in the published literature these models are among the few suitable for fatigue assessment of masonry elements under repeated normal stresses. By comparing the chosen models, it possible to conclude that the model proposed by Casas (2009) actually represents the most comprehensive one, since it has been derived from the experimental results of Roberts et al. model (2006) with a probabilistic fashion, in line with the design philosophy adopted by many codes, including the EC3 (2003) and the Italian NTC-08 code (2008). Moreover, in the experimental campaign carried out by Roberts et al. (2006) the influence of stress gradient and saturation degree (dry, wet and submerged conditions) on the quasi-static and high-cycle fatigue strength of brick masonry was investigated, too. Differently from the Ronca et al. (2004) model (derived by imposing a small variation of the alternating loads), both Roberts et al. (2006) and Casas (2009) models estimate, at a number not too high of cycles, fatigue strengths ratios (Smax/Su) significantly very lower than 0.5, that is the value usually indicated as the fatigue endurance limit. This demonstrates the importance of an appropriate evaluation of the fatigue strength that may lead, if simplified methods are applied (such as the endurance limit criterion), to an overestimation of the actual fatigue strength. The fatigue assessment has regarded the brick masonry arches of a case study in Italy, an ancient multi-span masonry bridge still in service. The obtained results highlight that, in according to the stress-life curves adopted, in the actual condition the main arches

are characterized by very low fatigue strength and residual service life, resulting, at most, of about five years. As obtained with the numerical investigations, the application of CFRP wraps produces a significant benefit only on the ultimate carrying capacity, and especially in the case of intradosal application with good anchorage condition. On the contrary, no variation is produced on the fatigue strength and, consequently, on the arch residual service life. The crucial point in the applied fatigue assessment procedure becomes the choice of the most suitable stress-life curve. It must be marked, however, that in this study the considered ones have been derived from laboratory tests performed on masonry specimens having compressive strength values higher than the usual ones encountered in the existing masonry. Therefore, their application in the case of ancient brick masonry results inappropriate leading, as obtained in the case study, to opposite results. By assuming a high material knowledge level (KL3), it has been estimated an infinite residual service life of the main arch. By contrast, for the same arch if one considers a low masonry knowledge level (KL1) the residual service life is very low or even null. For this reason in future it is necessary, without any doubt, to define more appropriate and realistic stress-life curves, experimentally established for low compressive strengths, closer to the ones characterizing the existing brick masonry. To this aim particular attention should be also paid to the influence on the fatigue capacity of the cyclic load frequency.

As a matter of fact, the fatigue models examined in this study have been proposed for cycled loads having frequencies (more than 1 Hz) higher than the ones associated to traffic loads indicated into the considered codes (for example, in the case analyzed the traffic load frequency results equal to 0.015 Hz). Finally, the new laboratory tests will also permit to deeply study the fatigue behavior of masonry strengthened by externally bonded FRP wraps that is, to date, another research topic not yet duly investigated.

REFERENCES

BD 21/93. The assessment of highway bridges and structures, The Highways Agency HMSO. London, 1993.

BS EN998-2, 2003. Specification for mortar for masonry. Masonry mortar, British Standard Institution.

Casas J.R., 2009. A probabilistic fatigue strength model for brick masonry under compression, Journal of Construction and Building Material, Vol. 23(8), pp. 2964–2972.

Chen J. F., 2002. Load-bearing capacity of masonry arch bridges strengthened with fibre reinforced polymer composites, Advances in Structural Engineering, Vol. 5(1), pp. 37-44.

Clark G.W., 1994. Bridge analysis testing and cost causation project: serviceability of brick masonry, British Rail Research Report LR CES 151.

CNR-DT 200 R1/2013. Istruzioni per la Progettazione, l'Esecuzione ed il Controllo di Interventi di Consolidamento Statico mediante l'utilizzo di Compositi Fibrorinforzati, Materiali, strutture di c.a. e di c.a.p., strutture murarie. (In italian).

D.M. 14 Gennaio 2008. "Norme Tecniche per le Costruzioni", pubblicato su S.O. n. 30 alla G.U. 4 Febbraio 2008, n. 29 (In italian).

de Felice G., 2009. Assessment of the load-carrying capacity of multi-span masonry arch bridges using fibre beam elements, Engineering Structures, Vol. 31, pp. 1634–1647.

EN 1991-2:2003. Eurocode 1. Actions on structures – Part 2: Traffic loads on bridges.

EN 1993-1-9:2003. Eurocode 3. Design of steel structures – Part 1-9: Fatigue.

EN 1998-3:2004. Eurocode 8. Design of structures for earthquake resistance– Part3: Assessment and retrofitting of buildings.

Foraboschi P., 2004. Strengthening of masonry arches with fiber-reinforced polymer strips, ASCE Journal Composite Construction, Vol. 8(3), pp. 191–202.

Gelfi P., 2002. Role of Horizontal Backfill Passive Pressure on the Stability of Masonry Vaults, International Journal for Restoration of Buildings, Aedificatio Verlag, Freiburg, Vol. 8(6), pp. 573-589.

Italian Design Code Instructions (NTC-08 Instructions). Circolare 2 Febbraio 2009, n. 617 – Istruzioni per l'applicazione delle Nuove Norme Tecniche per le Costruzioni di cui al D.M. 14 gennaio 2008, pubblicata su S.O. n. 27 alla G.U. 26 Febbraio 2009, n. 47. (In italian).

Italian Transport Classification, 1992. D.L. 30 April 1992, n. 285 - Nuovo codice della strada." Pubblicato sul supplemento ordinario n.74 alla "Gazzetta Ufficiale" n. 114 del 18 maggio 1992 – Serie generale quanto definito da: "Nuovo codice della strada". (In italian).

Laterza M., D'Amato M., Casamassima V.M., 2016. Seismic performance evaluation of a multi-span existing masonry arch bridge. The Open Construction & Building Technology Journal, (Under review).

Laterza M., D'Amato M., Casamassima V.M, 2017. Stress-Life Curves Method for Fatigue Assessment of Ancient Brick Arch Bridges. International Journal of Architectural Heritage just-accepted (2017).

Melbourne C., Tomor A.K., Wang J., 2004. Cyclic load capacity and endurance limit of multi-ring masonry arches, In "Arch Bridge '04" Conference Proceedings, Barcelona, pp. 375-384.

OpenSees, 2009. Open System for Earthquake Engineering Simulation, http:// opensees.berkeley.edu.

Ronca P., Franchi A., and Crespi P., 2004. Structural failure of historic buildings: masonry fatigue tests for an interpretation model, Proceeding Paper of the Fourth International Conference on Structural Analysis of Historical Constructions (Bologna, Italy), pp. 273-279.

Roberts T. M., Hughes T. G., Dandamudi V. R., Bell B., 2006. Quasi-static and high-cycle fatigue strength of brick masonry, Journal of Construction and Building Material, Elsevier, Vol. 20(2006), pp. 603–614.